Expanded View Figures

Figure EV1. Examination of MIG-6 genetic alterations in different breast cancer subtypes.

A cBioPortal was used to access and visualize TCGA data for MIG-6 (*ERRFI1*) gene expression in 321 luminal and 58 HER2-enriched breast cancer subtypes. Each column represents an individual sample. The table at the bottom summarizes the frequency (%) of genetic alterations of the MIG-6 gene in different breast cancer subtypes.

B Box plots show the MIG-6 (*ERRFI1*) gene expression in different breast tumor subtypes in the Bertucci dataset of 266 primary breast cancer carcinomas, analyzed using Illumina HumanWG-6_v3 Arrays. The gene expression levels are determined using the R2 platform. In the box plot, error bars are the 95% confidence interval, the bottom and top of the box are the 25^{th} and 75^{th} percentiles, the line inside the box is the 50^{th} percentile (median), and any outliers are shown as open circles. $^{**}P < 0.01$, by Student's *t*-test.

C The bar graph shows the wide distribution of MIG-6 protein expression across the 85 tumor samples used for IHC staining.

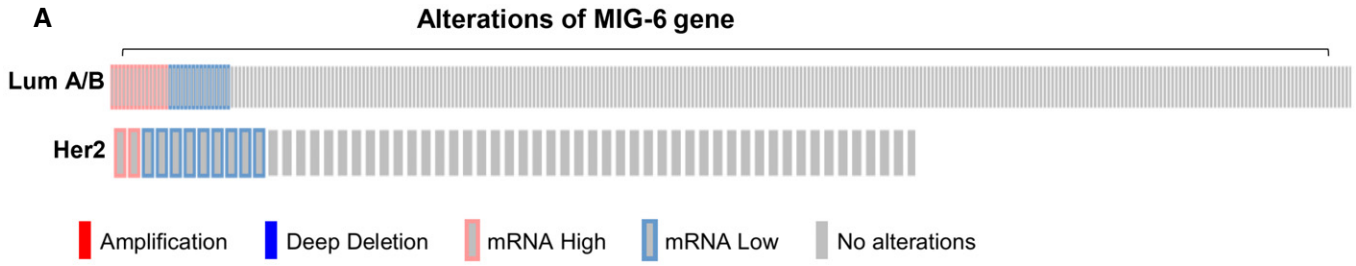

Summary of *ERRFI1* (MIG-6 gene) alteration

Percentage	upregulation/amplification	downregulation/deletion	total cases
Luminal A/B	5%	5%	321
Her2 enriched	3%	16%	58
Basal	19%	3%	81

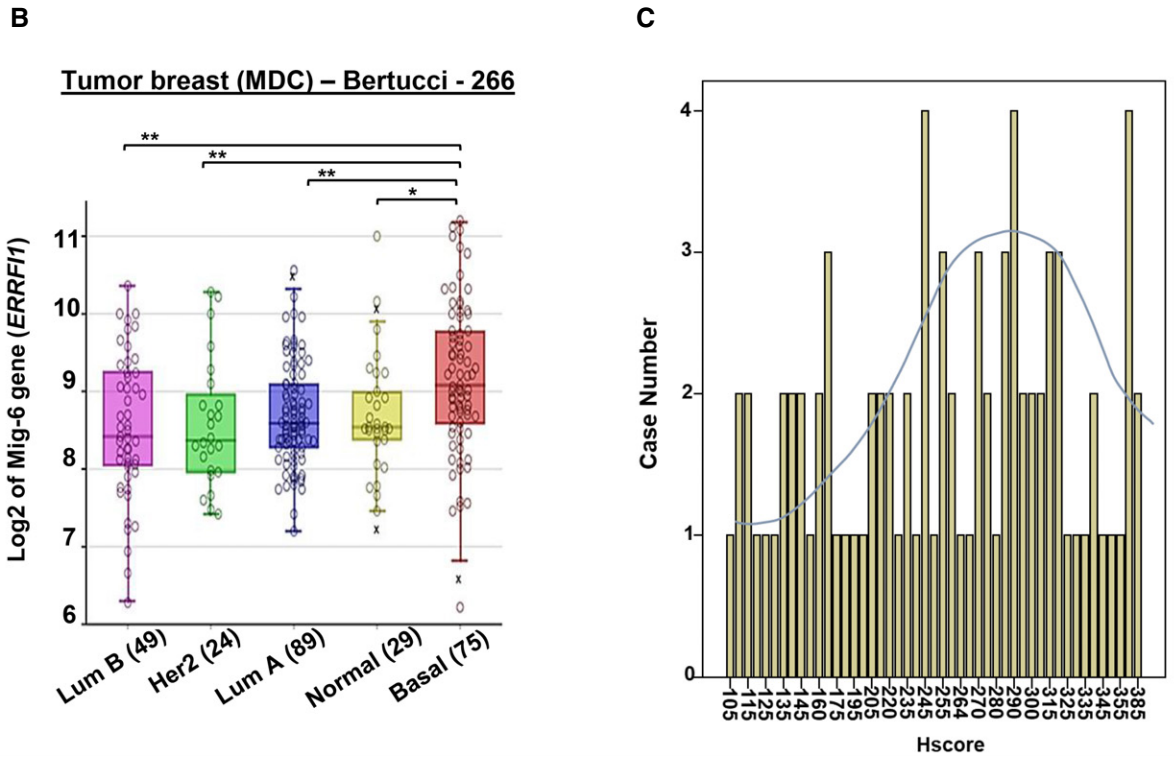

Figure EV1.

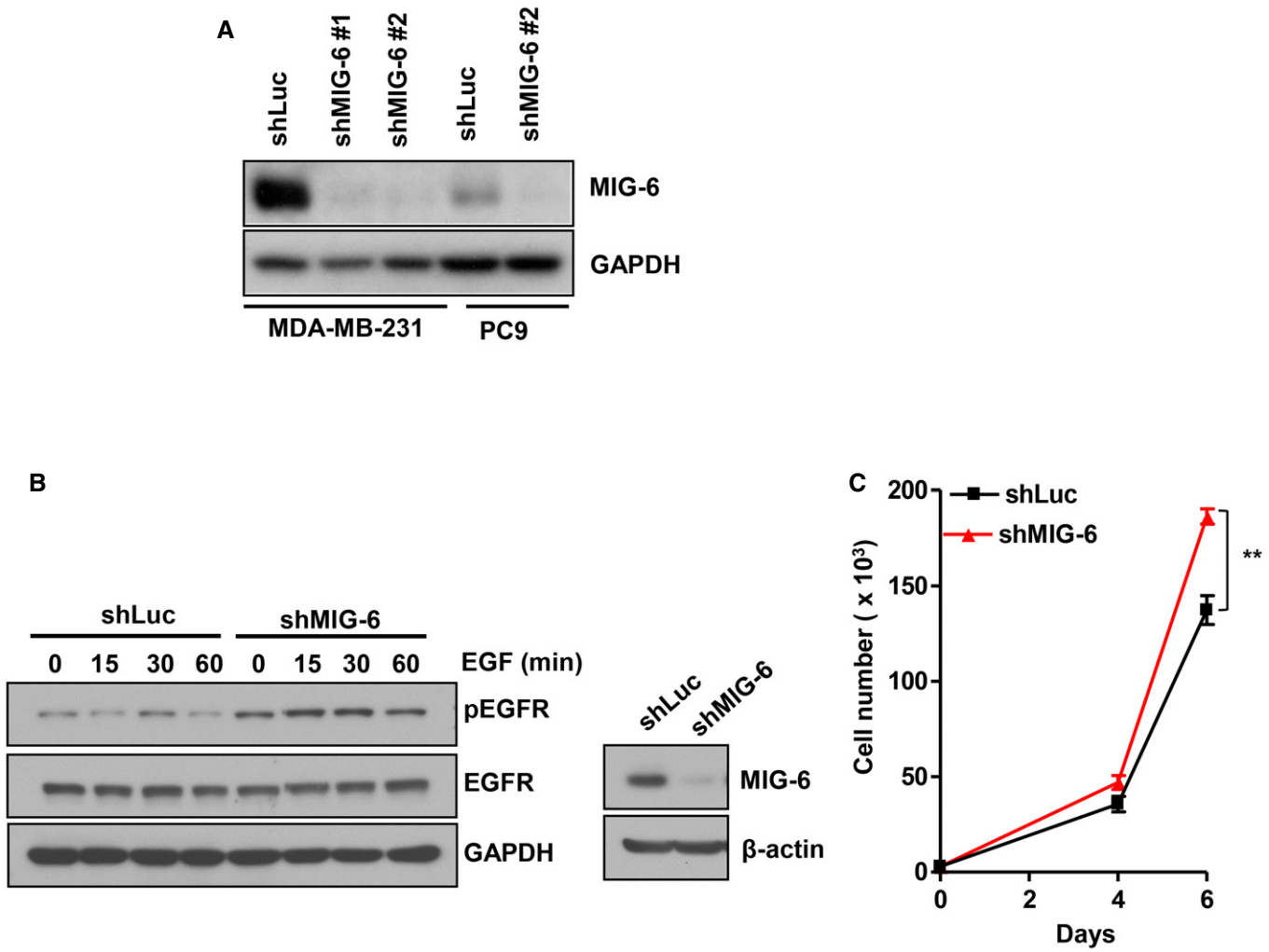

Figure EV2. MIG-6 deficiency promotes EGFR signaling and cell growth in lung cancer cells.

A Immunoblotting analysis for MIG-6 expression in Luciferase and MIG-6 knockdown MDA-MB-231 and PC9 cells.

B Immunoblotting analysis for phosphorylation and protein expression of EGFR in Luciferase and MIG-6 knockdown PC9 cells. Cells were serum-starved, treated with EGF for various time periods, and harvested for immunoblotting analysis.

C Cell proliferation and immunoblotting assays in Luciferase and MIG-6 knockdown PC9 cells ($n = 3$). The quantified results are presented as mean ± SD. $^{**}P < 0.01$, by Student's *t*-test.

Figure EV3. MIG-6 reprograms glucose metabolism toward glycolysis.

A Immunoblotting analysis for MIG-6 expression in breast cancer cells under normoxia (N) and hypoxia (H).

B Oxygen consumption rate (OCR) in BT549 cells with GFP or MIG-6 knockdown ($n = 15$; biological replicates).

C Quantitative results for basal OCR in the GFP and MIG-6 knockdown BT549 cells indicated by the orange box in Fig EV3B ($n = 15$).

D Quantitative results for maximal OCR in the GFP and MIG-6 knockdown BT549 cells indicated by the green box in Fig EV3B ($n = 15$).

E Histograms show the percentage of up/downregulated genes in the pentose phosphate pathways (left), gluconeogenesis (middle), and glycogen metabolism pathways (right) whose expressions were affected by MIG-6 knockdown in BT549 cells. For each gene, the change was calculated based on the equation: (shGFP-shMIG6)/shMIG-6 ($n = 3$).

F Lactate production assay in MDA-MB-231 cells with Luciferase or MIG-6 knockdown ($n = 3$).

G Lactate production assay in GFP and MIG-6 knockdown BT549 cells with or without gefitinib treatment for 72 h ($n = 3$).

Data information: The quantified results are presented as mean ± SEM. $^{*}P < 0.05$, $^{**}P < 0.01$, by Student's *t*-test.

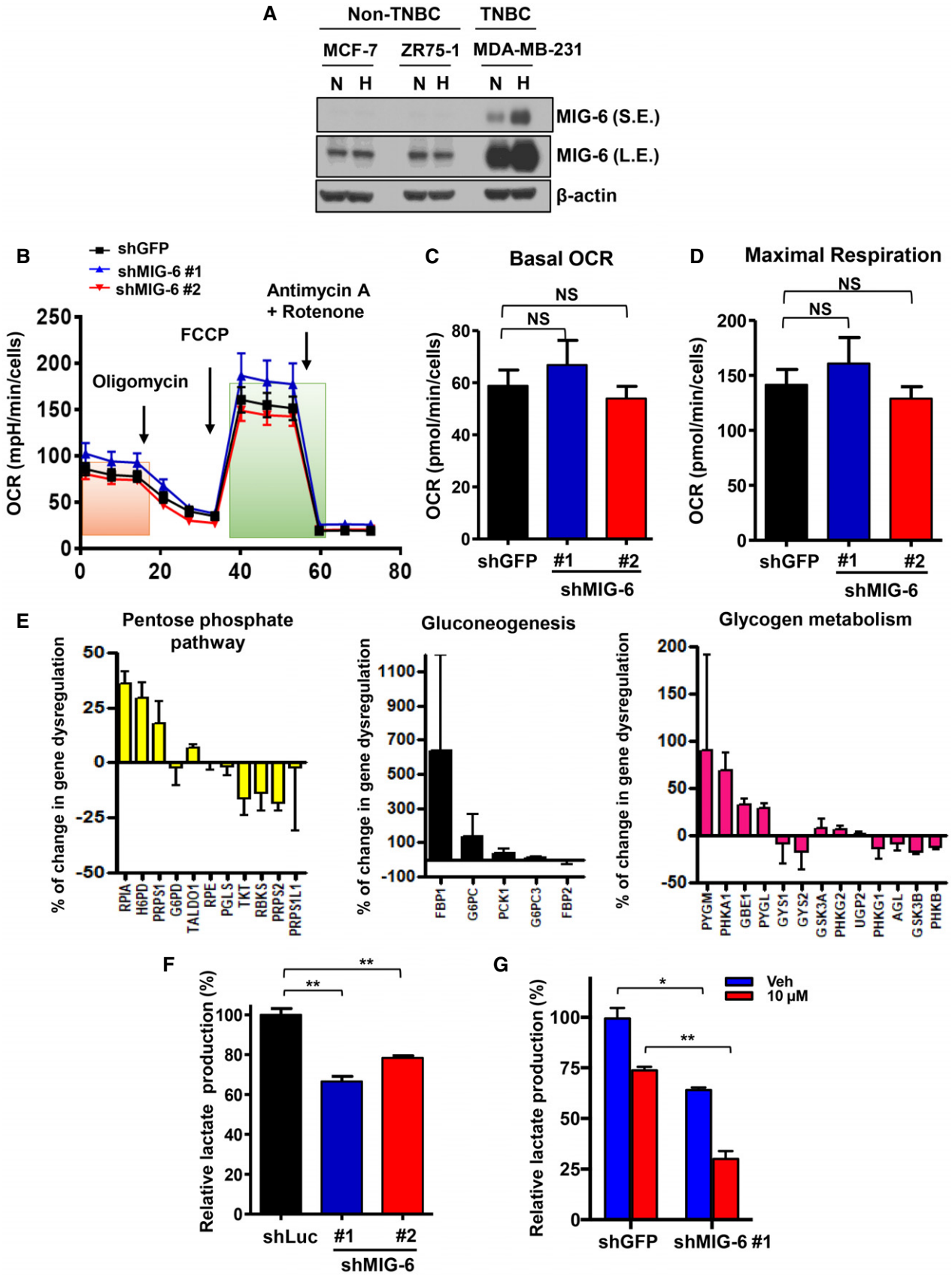
A
Non-TNBC
TNBC
MCF-7
ZR75-1
MDA-MB-231
N H N H N H
MIG-6 (S.E.)
MIG-6 (L.E.)
β-actin
B
shGFP
shMIG-6 #1
shMIG-6 #2
Antimycin A + Rotenone
FCCP
Oligomycin
OCR (mpH/min/cells)
C
Basal OCR
OCR (pmol/min/cells)
NS
shGFP #1 #2
shMIG-6
D
Maximal Respiration
E
Pentose phosphate pathway
% of change in gene dysregulation
RPIA H6PD PRPS1 G6PD TALDO1 RPE PGLS TKT RBKS PRPS2 PRPS1L1
Gluconeogenesis
FBP1 G6PC PCK1 G6PC3 FBP2
Glycogen metabolism
PYGM PHKA1 GBE1 PYGL GYS1 GYS2 GSK3A PHKG2 UGP2 PHKG1 AGL GSK3B PHKB
F
Relative lactate production (%)
shLuc #1 #2
shMIG-6
G
Veh
10 μM
shGFP shMIG-6 #1

Figure EV3.

Figure EV4. MIG-6 depletion reduces the expression of GLUT1.

A Box plots show the GLUT1 (*SLC2A1*) gene expression in different breast tumor subtypes in the Bertucci dataset of 266 primary breast cancer carcinomas, analyzed using Illumina HumanWG-6_v3 Arrays. The gene expression levels are determined using the R2 platform. In the box plot, error bars are the 95% confidence interval, the bottom and top of the box are the 25^{th} and 75^{th} percentiles, the line inside the box is the 50^{th} percentile (median), and any outliers are shown as open circles. $^{**}P < 0.01$, by Student's *t*-test.

B Immunoblotting analysis for GLUT1 protein expression in MDA-MB-231 cells with GFP or MIG-6 knockdown.

C Immunoblotting analysis for GLUT1 expression in the membrane and cytosolic fractions in BT549 cells with GFP or MIG-6 knockdown. EGFR and α-Tubulin served as markers for membrane and cytosolic fractions, respectively.

D Immunoblotting analysis for GLUT1 expression in the membrane and cytosolic fractions of MDA-MB-231 cells with Luciferase or MIG-6 knockdown.

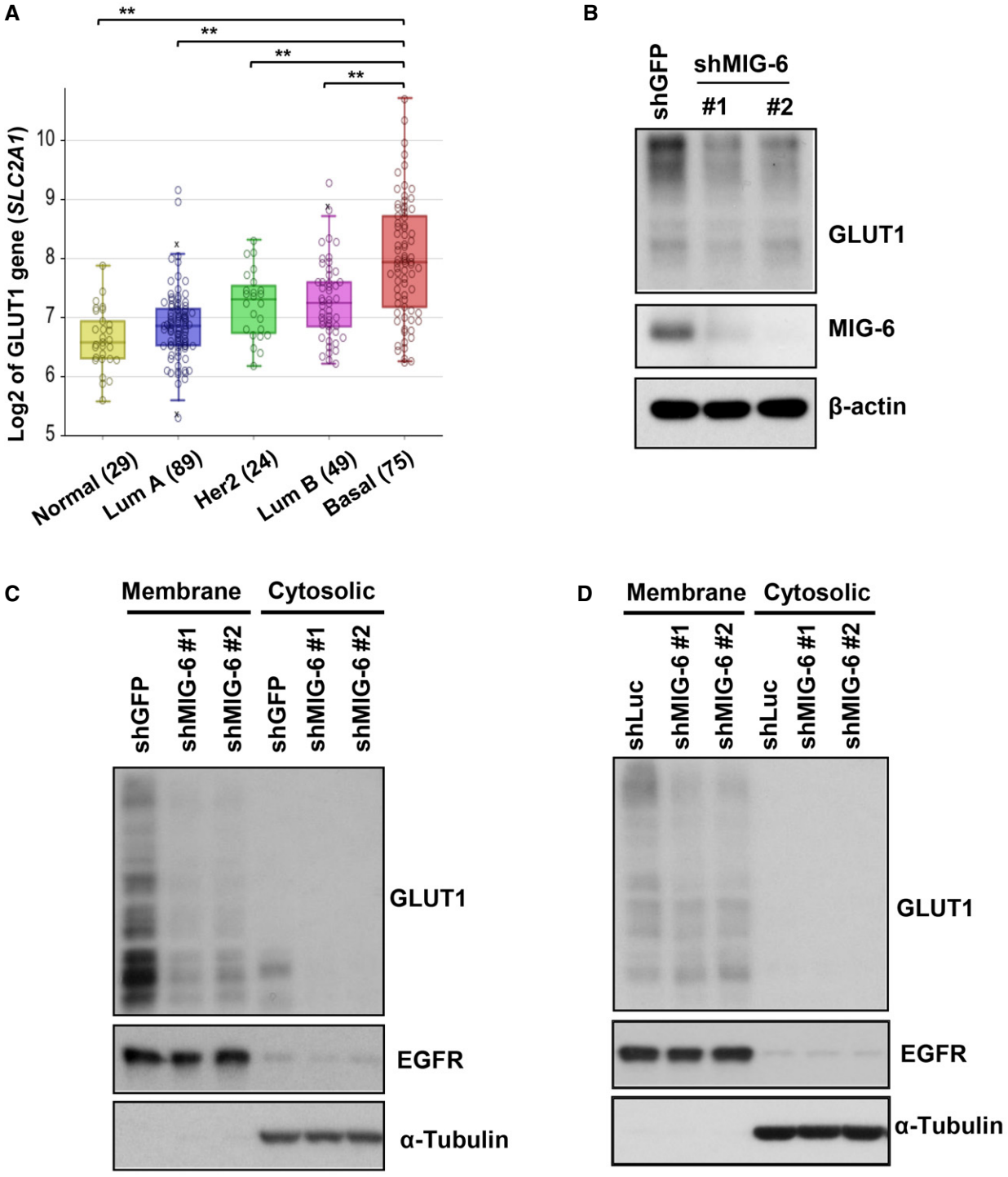

Figure EV4.

Figure EV5. Characterization of the mechanism by which MIG-6 regulates GLUT1 expression.

A Immunoblotting analysis for HIF1α expression in various breast cancer cells under normoxia (N) and hypoxia (H).
B Immunoblotting analysis for cMyc protein expression in BT549 cells with GFP or MIG-6 knockdown.
C Immunoblotting analysis for cMyc protein expression in MDA-MB-231 cells with GFP or MIG-6 knockdown.
D Immunoblotting analysis for HIF1α expression in response to MG132 treatment in BT549 cells with GFP or MIG-6 knockdown.
E GFP and MIG-6 knockdown BT549 cells transfected with the indicated plasmids were treated with MG132, subjected to immunoprecipitation with the HA-tag antibody, followed by immunoblotting analysis.
F Luciferase and MIG-6 knockdown BT549 cells were transfected with the indicated plasmids and subjected to MG132 treatment. Afterward, cells were harvested for IP with the HIF1α antibody, followed by immunoblotting analysis to determine the level of K48-linked ubiquitination of HIF1α.
G The upper panel shows an immunoblotting analysis for the half-life of the HIF1α protein in BT549 cells with GFP or HAUSP knockdown upon cycloheximide (CHX) treatment. The relative intensities of HIF1α protein expression are quantified by ImageJ software and normalized to that in shGFP cells without CHX. The lower panel shows the quantitative results for the half-life of the HIF1α protein in BT549 cells with GFP or HAUSP knockdown. The relative intensities of HIF1α protein expression quantified by ImageJ software are normalized to that in shGFP or shHAUSP cells without CHX treatment. The dotted line indicates 50% abundance of HIF1α, and the half-life ($t_{1/2}$) HIF1α protein.
H Quantitative result for the half-life of the HIF1α protein upon MIG-6 overexpression in BT549 cells with GFP or HAUSP knockdown upon CHX treatment. The relative intensities of HIF1α protein expression quantified by ImageJ software are normalized to that in each group without CHX treatment. The dotted line indicates 50% abundance of HIF1α, and the half-life ($t_{1/2}$) HIF1α protein.

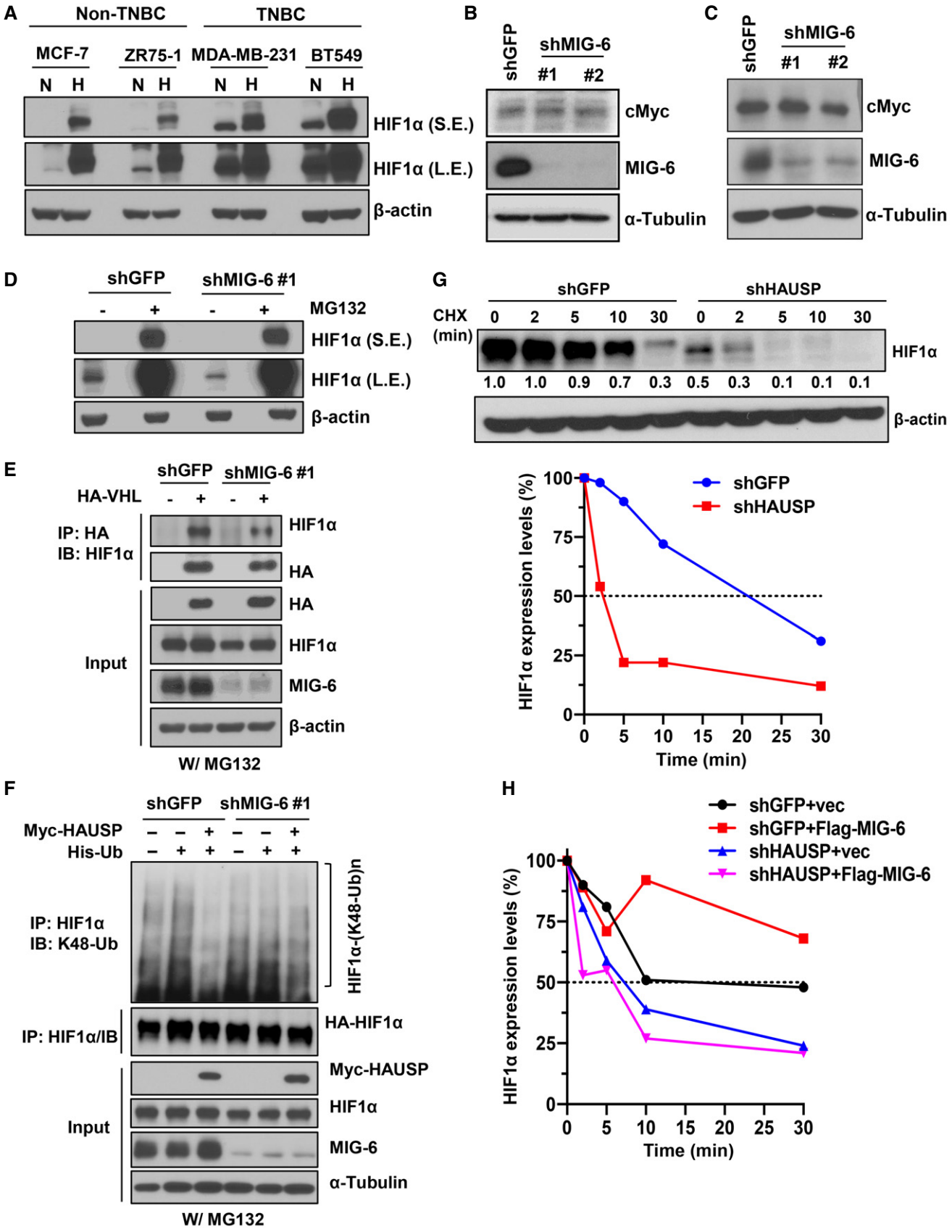
A
Non-TNBC
TNBC
MCF-7
ZR75-1
MDA-MB-231
BT549
N H N H N H N H
HIF1α (S.E.)
HIF1α (L.E.)
β-actin
B
shGFP
shMIG-6
#1 #2
cMyc
MIG-6
α-Tubulin
C
shGFP
shMIG-6
#1 #2
cMyc
MIG-6
α-Tubulin
D
shGFP
shMIG-6 #1
- + - +
MG132
HIF1α (S.E.)
HIF1α (L.E.)
β-actin
G
shGFP
shHAUSP
CHX (min) 0 2 5 10 30 0 2 5 10 30
HIF1α
1.0 1.0 0.9 0.7 0.3 0.5 0.3 0.1 0.1 0.1
β-actin
E
shGFP
shMIG-6 #1
HA-VHL - + - +
IP: HA
IB: HIF1α
HIF1α
HA
Input
HA
HIF1α
MIG-6
β-actin
W/ MG132
HIF1α expression levels (%)
Time (min)
shGFP
shHAUSP
F
shGFP
shMIG-6 #1
Myc-HAUSP – – + – – +
His-Ub – + + – + +
IP: HIF1α
IB: K48-Ub
HIF1α-(K48-Ub)n
IP: HIF1α/IB
HA-HIF1α
Input
Myc-HAUSP
HIF1α
MIG-6
α-Tubulin
W/ MG132
H
shGFP+vec
shGFP+Flag-MIG-6
shHAUSP+vec
shHAUSP+Flag-MIG-6
HIF1α expression levels (%)
Time (min)

Figure EV5.